Effect of hydrogen and oxygen on stainless steel nitriding

C. A. Figueroa, D. Wisnivesky, and F. Alvarez[a)]
Instituto de Física "Gleb Wataghin," Unicamp, 13083-970, Campinas, São Paulo, Brazil

(Received 27 December 2001; accepted for publication 17 April 2002)

The influence of hydrogen and oxygen on stainless steel implanted by nitrogen low-energy ions is systematically studied. It is shown that hydrogen intervenes moderately in the process only when the oxygen partial pressure in the deposition chamber is relatively high. For very low-oxygen partial pressures, the energetic nitrogen molecules impinging on the substrate sputter the thin oxide layer formed on the substrate. This allows the growing of a rich nitrogen layer beneath the surface, improving the diffusing of the implanted atom deeper in the bulk material. For higher-oxygen partial pressures, the sputtering is ineffective, and an oxide layer partially covers the surface even in the presence of hydrogen. The maximum depth penetration of nitrogen depends on the degree of oxygen coverage, which is fairly well described by a Langmuir absorption isothermal. Hardness depth profiling is consistent with the existence of a diffusion barrier formed by the oxygen absorbed on the surface. In order to understand the role of hydrogen on the nitriding process, samples preimplanted with hydrogen were subsequently treated with nitrogen and the hardness depth profiling analyzed. These results may provide a clue about the practical consequences of oxygen and hydrogen on the nitriding process. © *2002 American Institute of Physics.* [DOI: 10.1063/1.1483893]

I. INTRODUCTION

Stainless steel (SS) is extensively used in industrial applications due to its excellent corrosion resistance and in spite of its relative low load-bearing capacity. However, in the past decade, the development of plasma nitriding technologies have improved the wear resistance and hardness of these materials, making it attractive for applications demanding more stringent mechanical performance.[1–3] In general, nitriding processes use different plasma conditions and gaseous mixtures of nitrogen, argon, and hydrogen to optimize the mechanical properties of the material surface.[4–14] The extensive work done on the subject leads to a relatively thorough understanding of the nitriding process and the properties of the nitrated surface layer. However, a careful analysis of the bibliography on the subject shows an inconclusive response with regard to the hydrogen and oxygen roles on the depth and properties of the nitrated layer.[15,16] Roughly speaking, it is generally accepted that for a given process temperature, hydrogen enhances nitrogen diffusion by reducing the surface oxide layer ("diffusion barrier").[17–19] However, the variety of nitriding techniques (e.g., pulsed plasma, glow discharge, gaseous nitriding, etc.) and conditions used in the experiments (e.g., background pressure, ion current density, ion energy, gaseous mixture, substrate temperature, etc.) prevent general conclusions about the key parameters influencing the final properties of the treated surface.

In an attempt to understand the main factors determining the characteristic of treated layers, one can analyze and compare results obtained with nitriding processes grouped according to the applied techniques. In experiments performed in pulsed-direct current (DC) plasma nitriding, adding hydrogen to the gaseous mixture *reduces* the diffusion of the nitrogen on stainless steel.[20] A similar effect of hydrogen was reported on nitrogen-treated SS using DC glow-discharge processes.[21] On the other hand, results obtained with rf-plasma nitriding processes in SS 316 suggest that hydrogen increases the nitrogen diffusion length of nitrogen.[17,18] Also, this trend was reported in low-alloy steel (31CrMoV9 steel) treated by microwave plasma.[22,23] Using arc discharge plasma, the addition of hydrogen apparently has no effect on the nitrated layer formed in SS 316.[24] However, almost 30 years ago, Hudis[25] reported modifications of the plasma structure due to the presence of hydrogen influencing the nitriding process. Hovorka *et al.*,[22] Renevier *et al.*,[24] and Ricard[26] studied the influence of the excited species present in the plasma and their influence on the material properties. In a theoretical study, Szasz *et al.*[27] concluded that small amounts of absorbed hydrogen are necessary to guarantee an efficient hardening effect. More recently, a fine comprehensive study using rf-plasma technique proved that hydrogen has an important role on the process by increasing the density of active nitriding species in the plasma.[28]

Many of these inconclusive results are due to the difficulty of controlling independently the parameters involved in the nitriding processes. Therefore, in order to overcome this inconvenience, we studied the effect of hydrogen and oxygen on SS 316 using an ion beam implantation gun (Kaufman cell).[29] In this type of ion source, the ion energy, current density, and ion species bombarding the material are accurately and independently controlled. Taking advantage of these possibilities, we systematically study ion nitrogen implantation on SS 316 controlling the ion energy, current density, and the nitrogen-hydrogen mixtures used to generate the plasma in the ion cell. The chamber oxygen partial pressure was carefully controlled by intentionally introducing an oxygen leak.

a)Author to whom correspondence should be addressed; electronic mail: alvarez@ifi.unicamp.br

Surprisingly, at very low-oxygen partial pressure ($<2\times10^{-5}$ Pa), a *pure ion hydrogen* ("prehydrogenation") bombardment produces *per se* modifications on the structure of the material, an effect normally neglected in standard nitriding process where hydrogen-nitrogen gaseous mixture are used.

At low-oxygen partial pressure, the tiny oxidized layer formed on the surface is sputtered away, without interference in the nitrogen diffusion into the bulk material. At higher-oxygen pressure, sputtering is inefficient and the oxidized layer prevents an efficient penetration of nitrogen.

At intermediate oxygen partial pressure, the presence of hydrogen in the ion beam increases the total nitrogen penetration in the bulk of the material, neutralizing the effect of oxygen, and modifying the hardness profile. It was found that hardness depth profile is compatible with oxygen Langmuir[30] isothermal absorption mechanisms. Finally, the morphology and the thickness of the nitrated layers were analyzed by scanning electron microscopy (SEM) and x-ray glancing diffraction measurements.

II. EXPERIMENT

Rectangular samples of 20×10 mm and 1-mm thick from the same AISI 316 stainless steel source were used for all the studies. The treated samples were mirror polished using standard metallurgical techniques. The nitriding experiments were performed in an ion beam apparatus with a 3-cm diameter DC Kaufman ion source. More detailed descriptions of the implantation system are found elsewhere.[31] The gases were introduced in the Kaufman ion source through mass flow-meter controllers and the ions impacted normal to the surface samples. The chamber pressure was monitored using a Varian cold cathode gauge and the pressure absolute values obtained using the gas correction factor provided by the manufacture.[32] This correction factor essentially depends on the ionization cross section of the gas.

The nitriding condition, from now on "standard," were: 60 min implantation using a pure nitrogen ion beam; $<10^{-4}$ Pa background pressure; 0.6 KeV ion energy; 380 ±10 °C substrate temperature, and 5.7 mA/cm^2 ion current. Nitriding experiments using a nitrogen-hydrogen ion beam were performed as follows. First, the Kaufman source was prepared to deliver 5.7 mA/cm^2, i.e., "standard" condition. Second, hydrogen was introduced into the Kaufman cell, increasing the total current to the desire value. In this way, the offer of nitrogen ions is assumed to be constant and the extra current stems from ionized hydrogen molecules.

In order to study the effect on nitrogen diffusion in hydrogen preimplanted materials, special substrata were prepared. Two prehydrogenated samples were prepared by irradiating the substrata for 30 and 75 min, respectively. The conditions were: 380 °C substrate temperature, 1 KeV ion energy, and 5.7 mA/cm^2 hydrogen ion beam current density. After hydrogen implantation, the samples were maintained (annealed) during 30 min at 380 °C in a 4×10^{-1} Pa hydrogen atmosphere. In all experiments, the current density was estimated by dividing the nominal beam current of the Kaufman ion source by the geometrical beam area.

TABLE I. High-vacuum nitriding experimental conditions used during deposition: background pressure: $<10^{-4}$ Pa; oxygen partial pressure (pp): $<2\times10^{-5}$ Pa; nitrogen pp: 1.1×10^{-2} Pa; ion energy: 0.6 KeV; deposition temperature: 380±10 °C; implantation time: 60 min.

$H_2/(H_2+N_2)$ (%)	Hydrogen partial pressure (Pa)	Ion current density, (mA/cm^2)
0	···	5.7
25	1×10^{-3}	6.0
40	2.6×10^{-3}	6.2
57	6.2×10^{-3}	6.7
66	9.6×10^{-3}	7.0
72	1.2×10^{-2}	7.1

The oxygen leakage was introduced in the vacuum chamber by a dedicated feeding mass flow-meter controller. The hardness was obtained using a Berkovich diamond tip (*NanoTest-300*) at depths varying between 50 and 1800 nm and the results analyzed using the Oliver and Pharr method.[33] The indentation was perpendicular to the nitrated surface and the tip load controlled the penetration depth. Piling-up effects were not considered. The cross section of the nitrated layers was revealed by attacking the samples at room temperature with Marble's solution (10 g copper sulfate in 100 ml of 6 M hydrochloric acid) and measured by scanning electron microscopy (SEM/JEOL JMS-5900LV). The nitrated layer thickness was directly measured from the SEM images. The phases near to the surface layers were identified using glancing angle x-ray diffraction. The radiation used was the Cu K_α (λ=0.154 nm, U=50 KeV, and I=100 mA) line at an incident angle of 5°.

III. RESULTS

A. Hydrogen effect in high vacuum (HV) conditions

Table I shows the condition used in experiments performed at "high vacuum" (HV) ($<10^{-4}$ Pa), i.e., where the *residual* oxygen partial pressure is $<2\times10^{-5}$ Pa. Figure 1 shows the hardness versus depth for pure nitrogen and two different nitrogen-hydrogen mixtures implanted samples in

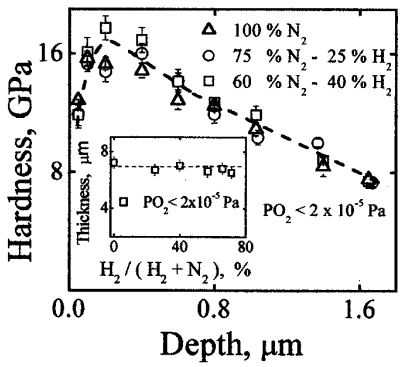

FIG. 1. Hardness vs depth obtained at different nitrogen-hydrogen mixtures. Inset: nitrated layer thickness obtained at different nitrogen-hydrogen mixtures used in the ion gun. All the experiments are performed at oxygen partial pressure $<2\times10^{-5}$ Pa. The lines are a guide for the eyes.

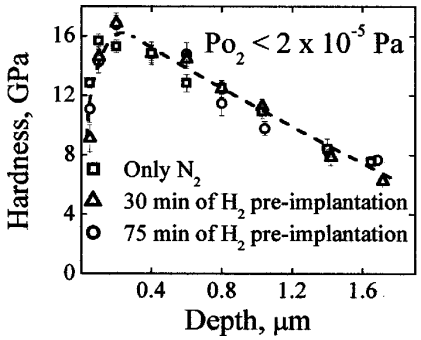

FIG. 2. Hardness vs depth obtained with a pure nitrogen ion beam. The lines are a guide for the eyes.

HV conditions. Figure 1, inset, shows that the total thickness of the nitrated layer *does not depend* on the hydrogen-nitrogen mixtures used on the material treatment. These results strongly suggest that hydrogen is not playing an important role on the final hardness profile of the nitrated layer provided that the oxygen partial pressure is "sufficiently low." For higher-oxygen partial pressures, on the other hand, hydrogen has a moderate effect on the nitrated layer properties such as the thickness and hardness profile (Sec. III C).

B. Effect of hydrogen preimplanted (HV conditions)

In an attempt to understand independently the effects of hydrogen on nitrogen diffusion, previously prepared substrata were nitrated in HV conditions, i.e., in those conditions where oxygen is not interfering with the final material hardness (see Secs. II and III A). Two types of samples prepared in HV are compared: (1) Samples prehydrogenated and subsequently nitrogen implanted in "standard" conditions and (2) samples implanted in "standard" conditions. In Fig. 2 we have plotted the results obtained with the prehydrogenated material. For the purpose of comparison, the curve of a "standard" sample from Fig. 1 is included. These results show that, *in HV conditions*, it is equivalent to treat the material with pure nitrogen or preimplanting hydrogen followed by nitrogen irradiation. Finally, the x-ray diffraction pattern of bare and prehydrogenated material are shown in Fig. 3.

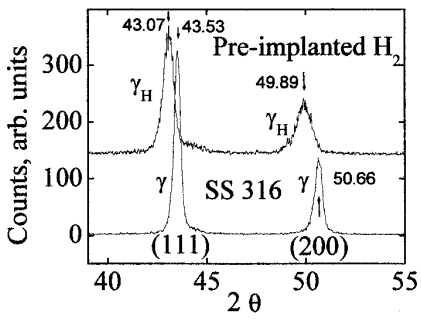

FIG. 3. X-ray diffraction pattern obtained at an angle of 5^0. Lower curve: untreated SS 316; upper curve: prehydrogenated substrate. The variation of the crystalline planes distances is 1.5% and 4.6% for the ⟨111⟩ and ⟨200⟩, respectively.

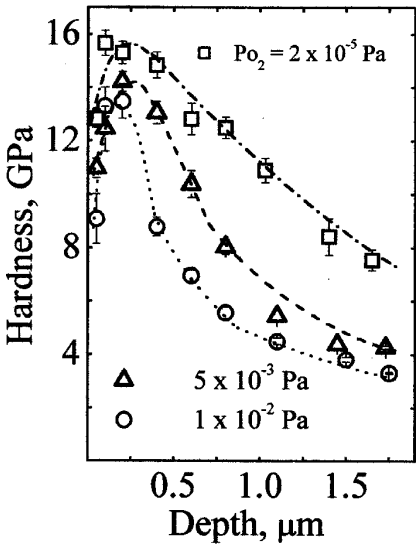

FIG. 4. Hardness vs depth obtained with three different background oxygen partial pressures using a pure nitrogen ion beam. The lines are a guide for the eyes.

C. Hydrogen effect in a controlled oxygen atmosphere

In order to study the differences observed when oxygen is present during implantation, experiments with several chamber gaseous mixtures were performed. Figure 4 shows the hardness versus depth of samples treated at three different background oxygen partial pressures with a pure nitrogen ion beam, i.e., "standard" conditions. Higher-oxygen partial pressure reduces the total nitrogen penetration. Figure 5 shows the total nitrogen depth penetration as a function of oxygen partial pressure implanted in "standard" conditions and with nitrogen-hydrogen mixture. As shown in Fig. 5, the

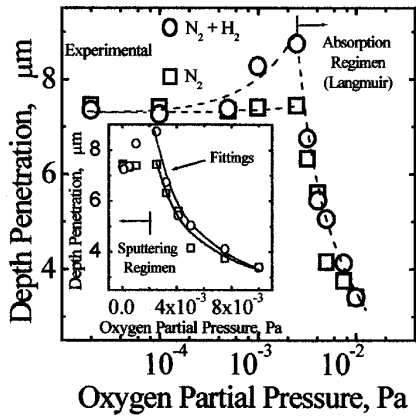

FIG. 5. Total nitrogen depth penetration vs oxygen partial pressure (pp) in the deposition chamber. Squares: implanted samples using pure nitrogen ion bean (nitrogen pp: 1.1×10^{-2} Pa; current density, cd: 5.7 mA/cm^2). Circles: implanted samples using nitrogen (pp: 1.1×10^{-2} Pa) and hydrogen (pp: 5×10^{-3} Pa); total ion beam density: 6.7 mA/cm^2. The dashed lines are a guide for the eyes. Inset: theoretical fittings (solid lines) using a Langmuir isothermal absorption law for pure (lower curve) and nitrogen-hydrogen (upper curve) implanted samples, respectively. Note the linear scale in the inset plot.

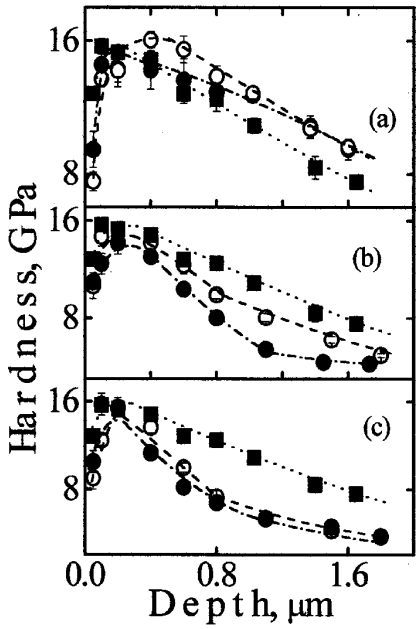

FIG. 6. Hardness vs depth profiles in samples treated with and without hydrogen in the ion beam at different chamber oxygen partial pressures, PO_2 (hollow circle, N_2+H_2; filled circle, N_2). (a) $PO_2=2.5\times10^{-3}$ Pa.; (b) $PO_2=5\times10^{-3}$ Pa, and (c) $PO_2=7.5\times10^{-3}$ Pa. All curves are compared with the hardness profile obtained at high vacuum ($PO_2<2\times10^{-5}$ Pa, filled squares). The dashed lines are a guide for the eyes.

nitrogen depth penetration decreases for oxygen partial pressures above 2.5×10^{-3} Pa, even in the presence of hydrogen. However, adding hydrogen to the ion source modifies the hardness profiles [Figs. 6(a)–6(c). For the purposes of comparison the hardness profiles of a sample implanted at $<2\times10^{-5}$ Pa oxygen partial pressure are included in the plot.

IV. DISCUSSION

The role of the oxygen on the surface process of nitrogen diffusion into the bulk at different implantation conditions has been the subject of several studies.[34,35] To understand these processes is crucial because the final properties of the nitrated material depend on the phenomena occurring on the surface. In order to gain physical insight into the effect of hydrogen and oxygen on the mechanical material properties during the nitriding process, we shall discuss the possible mechanisms responsible for the observed results. The mechanical properties obtained in the nitriding process depend on structural changes introduced by nitrogen. Indeed, the proportionality between hardness and nitrogen profile concentration is a well-established experimental result.[36,37] Therefore, in the following discussion we should bear in mind that the hardness profiles roughly represent the bulk nitrogen profile.

The nitriding process is a complex nonequilibrium phenomenon consisting of the interplay of three main factors, namely, gaseous mixture, type of solid, and ions species impinging on the sample. The process can be envisaged as occurring in three steps: (1) mass transfers from plasma phase to solid phase (ion implantation); (2) physical and chemical sputtering, physical and chemical adsorption (and desorption) from the gaseous mixture surrounding the metal surface (including uncontrolled residual gases such as water vapor and oxygen); and (3) diffusion into the bulk of formed complex and/or atomic molecular elements.

Several factors determine the final characteristics of the nitrated layer. Among the variety of species present in the chamber deposition, oxygen has a high-sticking factor to the metal surface. Therefore, a surface oxide is easily formed by dissociate adsorption (generally as Fe_2O_3) or chemical adsorption (chemisorptions), even at low-partial pressure.[38] The ions arriving at the surface are implanted and quickly neutralized. Subsequently, the species move into the material bulk by a complex mechanism involving diffusion and formation of compounds, i.e., with an average coefficient of diffusion strongly dependent on temperature. Finally, the ions impacting the substrate produce physical sputtering and chemical etching.

It is thought that hydrogen acts by saturating nitrogen traps and consequently increasing the species diffusion length. Indeed, the nitrogen diffusion length in SS is low when compared with nitrogen diffusion in standard steel due to the formation of chromium-nitrides compounds ("traps").[39,40] Therefore, in order to understand the role of hydrogen *per se* in the material structure, preimplanted samples were studied (see Sec. III B). It is interesting to remark that hardness profile of exclusively hydrogenated samples shows a moderated increment (~10%) in hardness as compared with plain SS (not shown). However, hardness depth profiling curves show that there are no important changes introduced by implanting nitrogen in prehydrogenated SS (Fig. 2). Sugiyama *et al.* reported similar results[41] by electrically introducing hydrogen in SS 316. It is interesting to note that the diffraction patterns of the prehydrogenated sample show a mild expansion of the γ phase (fcc) (Fig. 3). Therefore, the introduction of hydrogen produces, although minor, material modifications. Indeed, the moderate network expansion suggests that hydrogen will not appreciably change the nitrogen diffusion coefficient, a phenomenon intimately associated to the crystalline structure of the material. This probably explains why the hardness profiles are essentially the same to those obtained in samples irradiated in "standard" conditions, i.e., without hydrogen preimplantation. Strictly speaking, however, the prehydrogenated material should be considered modified since it was previously submitted to a sort of annealing. In other words, it is not equivalent to preimplant hydrogen bombarding afterwards with nitrogen than to bombard *simultaneously* the material with a beam containing nitrogen and hydrogen ions.

Using rf-plasma, Priest *et al.*[28] reported different results. These researchers found clear differences in material prepared as follows: (1) three-hour precleaned samples in pure hydrogen plasma nitriding afterwards the material in pure nitrogen plasma and (2) nitriding samples in pure nitrogen plasma. We note, however, that in rf plasma the energy of the ions impinging the work piece is determined by inelastic scattering. In a normal rf-plasma system this energy is ~50 eV,[35] a much lower value than used in this work (~1.0 KeV), diminishing the hydrogen ion penetration. Therefore, care

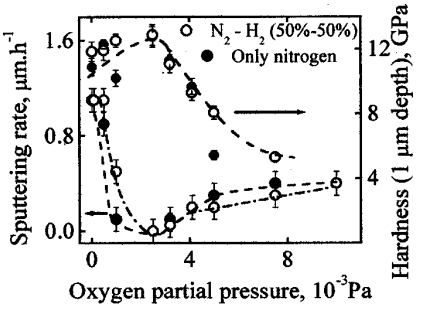

FIG. 7. Sputtering rate and hardness vs oxygen partial pressure. The dashed lines are a guide for the eyes.

must be exercised with the extension of our conclusions to different experimental situations.

As shown above (Sec. III C), implantation processes in atmospheres containing higher-oxygen partial pressures profoundly modified the hardness and thickness of the nitrated layer (Figs. 4, 5, and 6). The following trends are observed: (1) at low-oxygen partial pressures (2.5×10^{-3} Pa), adding hydrogen to the ion beam neutralized the effect of oxygen deep in the bulk material, improving considerably the hardness profile [Fig. 6(a)]; (2) at intermediate oxygen partial pressure (5×10^{-3} Pa), the presence of hydrogen recovers part of the hardness profile [Fig. 6(b)]. However, the effect is not enough so as to restore completely the profile obtained with the lower-oxygen partial pressure, i.e., 2×10^{-5} Pa; and (3) at higher-oxygen partial pressure (7.5×10^{-3} Pa) the effect of hydrogen is innocuous [Fig. 6(c)].

In the attempt to understand the origin of these effects it is interesting to discuss a possible physical model of the process. Considering quasiequilibrium, the oxygen present in the chamber is very well modeled by the classical kinetic theory of gases. The Maxwell theory of gases shows that the intensity of molecules impinging the surfaces, r_{IG}, at constant temperature is proportional to the oxygen partial pressure. The impinging molecule has some probability of being physically or chemically absorbed. The latter process occurs through the formation of metal oxides, mainly Fe_2O_3. Simultaneously with this process, part of the growing oxide layer is removed by sputtering. The oxide removal rate r_{SR} is proportional to the ion energy, ion flux, and sputtering yield.[42] In the presence of oxygen, the ratio $r_{IG}/r_{SR}>1$ allows the growing of a relatively thick oxidized layer, preventing a deeper nitrogen penetration (Fig. 5). Reducing the oxygen partial pressure is a route to diminish this ratio, i.e., $r_{IG}/r_{SR}<1$, as confirmed by Fig. 1. Also, it is expected that hydrogen will reduce the oxidized layer decreasing the r_{IG}/r_{SR} ratio and more efficient nitrogen diffusion obtained. We shall come back to this subject later on.

Figure 7 shows the sputtering rate and hardness (at 1 μm depth) versus oxygen partial pressure. The 1 μm depth was arbitrarily chosen for comparison purposes. Two main conclusions are obtained from this plot: (1) the sputtering rate depends on the beam composition and the chamber oxygen partial pressure. Moreover, the curve shows a minimum sputtering rate about 2×10^{-3} Pa oxygen partial pressure and (2) the hardness shows a "complementary" behavior, i.e., a maximum is obtained where the sputtering rate is negligible.

These conclusions suggest three implanting regimens: (R1) the "sputtering" regimen ($Po_2<1\times10^{-3}$ Pa), where the ion beam easily erodes the natural tiny oxidized layer. This diminishes considerably the potential barrier to nitrogen penetration improving nitrogen diffusion.[43–45] We remark, however, that in this regimen the metal is also eroded making thinner the final layer containing nitrogen ($r_{IG}/r_{SR}<1$); (R2) the high-oxygen partial pressure regimen ($Po_2>3\times10^{-3}$ Pa), where the attached oxygen forms a thick oxidized layer, blocking nitrogen diffusion. Indeed, in this regimen the sputtering is less important when compared to the one observed in the regimen R1, supporting the suggestion that the oxidized layer limits nitrogen penetration (Fig. 7); and (R3) the intermediate regimen ($\sim1\times10^{-3}$ Pa$<Po_2<\sim3\times10^{-3}$ Pa), with negligible sputtering and therefore the implanted nitrogen is retained. Moreover, in this regimen, the thin oxidized layer does not interfere appreciably with nitrogen diffusion.

In the regimen R1, sputtering prevents hydrogen retention on the metal surface making its presence almost irrelevant. In regimens R2 and R3, on the contrary, hydrogen plays a role on the hardness profile (Fig. 6). From a chemical point of view, it is expected that excited hydrogen atoms will reduce oxygen compounds, a reaction catalyzed by the metallic surface. Indeed, it is well known that transition metals (e.g., Pt) are very active catalyzing water reaction on its surface.[46,47] Therefore, it is expected that the thickness and composition of the oxidized layer will depend on the presence of hydrogen on a substrate containing a transition element such as iron. In an attempt to understand regimens R2 and R3, let us assume that the maximum nitrogen penetration, $\mathbf{d_N}$ at a fixed temperature (and time), is inversely proportional to the oxygen surface coverage σ

$$\mathbf{d_N}=\frac{\mathbf{k}}{\sigma}, \tag{1}$$

where $\mathbf{k}$ is a constant at a fixed temperature. This is a physically plausible assumption since, as observed in regimen R1, a less oxidized surface facilitates nitrogen diffusion in the material bulk. Also, we shall assume that σ follows a Langmuir isothermal absorption law[30]

$$\frac{\mathbf{1}}{\sigma}=\frac{\mathbf{1}}{\sigma_0}+\frac{\mathbf{1}}{\mathbf{b}\sigma_0\mathbf{P}}. \tag{2}$$

Here, $\mathbf{P}$ denotes the partial pressure of oxygen at the working condition, $\mathbf{b}$ is the temperature-dependent constant (adsorption–desorption relationship), and σ_0 is the surface coverage of one monolayer. The Langmuir isothermal $\theta=\sigma/\sigma_0$ represents the *coverage ratio* up to one monolayer formation system, i.e., a situation generally found at low pressure. In the present situation, the sputtering is also contributing to form a tiny oxidized over layer, a situation physically compatible with a Langmuir isothermal. Substituting Eq. (2) in Eq. (1)

$$\mathbf{d_N}=\frac{\alpha}{\mathbf{P}}+\gamma, \tag{3}$$

TABLE II. Adjusting parameters obtained by modeling the nitrated layer thickness by a Langmuir isothermal (Fig. 5).

	γ (μm)	α (μm Pa)	$P_0=\alpha/\gamma$ (Pa)
With hydrogen (H)	1.6±0.3	$(1.7\pm0.1)\times10^{-2}$	$(1.06\pm0.25)\times10^{-2}$
Without hydrogen (nH)	1.9±0.3	$(1.4\pm0.1)\times10^{-2}$	$(0.7\pm0.2)\times10^{-2}$

where $\alpha=\mathbf{k}/\mathbf{b}\sigma_0$ and $\gamma=\mathbf{k}/\sigma_0$ are adjustable parameters. The curves fitted by applying this model are displayed in Fig. 5 (inset, solid lines) showing a fairly good agreement with experimental data. The parameters obtained in the fitting are in Table II.

As discussed before, the effect of hydrogen on hardness profile is substantial at relatively high-oxygen partial pressures [Figs. 6(a) and 6(b)]. These results contrast with the lack of influence of hydrogen on the *total diffused* layer thickness (Fig. 7). However, we note that hardness gives an accurate measurement that is proportional to nitrogen depth, while the *total diffused* layer is not a spatially resolved technique.

Using Eq. (1), Eq. (3) can be written as follows:

$$\frac{\mathbf{k}}{\gamma\sigma}=\frac{\alpha}{\gamma\mathbf{P}}+\mathbf{1}=\frac{\mathbf{P_0}}{\mathbf{P}}+\mathbf{1}. \tag{4}$$

Comparing with Eq. (2), $\mathbf{P_0}=\alpha/\gamma=\mathbf{1/b}$ and $\sigma_0=\mathbf{k}/\gamma$. The parameter $\mathbf{P_0}$ is the oxygen partial pressure $\mathbf{P}$ giving a surface coverage $\theta_{1/2}=0.5$.

Substituting α and γ from Table II, the ratio $\mathbf{P_0^H/P_0^{nH}}\approx\mathbf{1.4\pm0.4}$ and $\sigma_0^{\mathrm{H}}/\sigma_0^{\mathrm{nH}}\approx\mathbf{0.9\pm0.4}$ is obtained. Here, **H** and **nH** stand for hydrogen and nonhydrogen presence in the ion beam. Therefore, the necessary oxygen pressure $\mathbf{P}$ to cover 50% of the surface ($\theta_{1/2}=0.5$) in the presence of hydrogen is ~40% higher than in the case of a pure nitrogen ion beam. Also, a different value of σ_0 indicates that the total coverage area is modified, i.e., fewer sites are available for oxygen by the presence of hydrogen. However, the error in the determination of σ_0 and $\mathbf{P_0}$ is considerably large and more work is necessary to improve the understanding of the phenomenon. Moreover, considering that these results stem from an ideal numerical model, they should be taken only as a trend to guide future experiments.

It is interesting to remark that the pulsed nitriding process occurs at higher-working pressure, where the ion mean free path is relatively small (~1–2 cm). As remarked above, the strong inelastic scattering of the nitrogen on the way to the metal surface reduces the ion energy to about 50 eV[35] making the sputtering negligible. In this condition, the hydrogen chemical etching decreases the efficiency of the oxidized blocking barrier, allowing the formation of a nitrogen-rich zone improving the nitrogen species diffusion into the material bulk. Indeed, hydrogen diminishes the necessity of strident vacuum conditions, a solution economically more attractive on an industrial scale. Last but not least, it is important to note that in pulsed plasma nitriding, the residual oxygen constitutes part of the ionized plasma, i.e., oxygen species are also implanted. On the other hand, the ion beam used in this work is composed only by nitrogen and/or hydrogen while oxygen is mainly neutral and with very low energies, i.e., ~kT. Therefore, care must be exercised when comparing results.

V. CONCLUSIONS

The effect of oxygen and hydrogen on the hardness properties of implanted SS 316 is reported. The presence of oxygen in the deposition chamber limits nitrogen diffusion in the material. It is shown that hydrogen plays a role on the material hardness enhancement only when oxygen partial pressure is relatively high. Three implantation regimens were identified: (R1) at low-oxygen vacuum pressure ($PO_2<2\times10^{-3}$ Pa) strong sputtering prevents the formation of a barrier oxidized layer acting as a diffusion barrier. However, the erosion of the implanted nitrogen layer partially diminishes the thickness of the nitriding layer. In this regimen the presence of hydrogen does not modify the hardness profile; (R2) a high-oxygen partial pressure ($PO_2>3\times10^{-3}$ Pa), where sputtering is moderated. In this regimen, the formation of a thick oxidized layer prevents efficient nitrogen diffusion even in the presence of hydrogen; and (R3) an intermediate oxygen partial pressure where the sputtering phenomenon is negligible. In this regimen, a superficial rich-nitrogen layer is formed enhancing the diffusion of nitrogen. The presence of hydrogen modifies the diffusion process, moderately enhancing the hardness profile.

The formation of the oxidized layers in regimens R2 and R3 is modeled assuming Langmuir absorption isothermals. In this model, the thickness of the nitrogen-containing layer depends on the oxygen coverage ratio. Adding hydrogen to the bombardment beam modifies the hardness profile by partially neutralizing the effect of oxygen. If hydrogen is present, the numerical fitting shows that ~40% higher-oxygen pressure is necessary to cover 50% of the surface. In regimen R2, only a moderately increasing nitrogen penetration is observed. This effect probably stems from the low-hydrogen retention due to the material sputtering. It is suggested that the low-energy ion (~50 eV), i.e., low-sputtering erosion involved in plasma-pulsed processes is the reason for the beneficial role of hydrogen in the process. Indeed, as shown in this work, in regimen R2 sputtering is not important. Therefore, more hydrogen is retained on the surface, reducing the oxidized layer, and thus facilitating nitrogen diffusion.

Prehydrogenated SS followed by nitrogen bombardment does not change the profile material hardness. This result challenges the reports that hydride formation ("trap quenching") improves hardness in nitrogen-hydrogen-treated SS. Finally, it is suggested that at adequate low-sputtering rate

and nitrogen-hydrogen ion beam bombardment it is possible to neutralize the effect of the diffusion barrier formed by surface oxidation.

ACKNOWLEDGMENTS

The authors are indebted to M. I. Romero, D. Ugarte, M. Bica, Erika Ochoa, and C. Ribeiro for helping with the measurements. This work was partially sponsored by FAPESP. C.A.F. and F.A. are Fapesp and CNPq fellows, respectively.

[1] A. H. Deutchman, R. J. Partyka, and C. Lewis, Conference Proceedings of the ASM-2nd International Conference, Cincinati, Ohio, edited by T. Spalvins and W. L. Kovacs, ASM, Matals Park, OH, 1989, p. 29.
[2] Z. L. Zhang and T. Bell, Surf. Eng. **1**, 131 (1985).
[3] F. El-Hossary, F. Mohammed, A. Hendry, D. F. Fabian, and Z. Szaszne-Csih, Surf. Eng. **4**, 150 (1988).
[4] M. K. Lei and Z. L. Zhang, J. Vac. Sci. Technol. A **13**, 2986 (1995).
[5] G. A. Collins, R. Hutchings, K. T. Short, J. Tendys, X. Li, and M. Samandi, Surf. Coat. Technol. **74–75**, 417 (1995).
[6] E. Menthe, K.-T. Rie, J. W. Schultze, and S. Simson, Surf. Coat. Technol. **74–75**, 412 (1995).
[7] R. Wei, J. J. Vajo, J. N. Matossian, P. J. Wilbur, J. A. Davis, D. L. Williamson, and G. A. Collins, Surf. Coat. Technol. **83**, 235 (1996).
[8] T. Bacci, F. Borgioli, E. Galvanetto, and G. Pradelli, Surf. Coat. Technol. **139**, 251 (2001).
[9] S. Mändl and B. Rauschenbach, Defect Diffus. Forum **188–190**, 125 (2001).
[10] A. Saker, Ch. Leroy, H. Michel, and C. Frantz, Mater. Sci. Eng., A **140**, 702 (1991).
[11] A. Leyland, D. B. Lewis, P. R. Stevenson, and A. Matthews, Surf. Coat. Technol. **62**, 608 (1993).
[12] M. Samandi, B. A. Shedden, T. Bell, G. A. Collins, R. Hutchings, and J. Tendys, J. Vac. Sci. Technol. B **12**, 935 (1994).
[13] B. Larisch, U. Brusky, and H.-J. Spies, Surf. Coat. Technol. **116–119**, 205 (1999).
[14] M. K. Lei and Z. L. Zhang, J. Vac. Sci. Technol. A **15**, 421 (1997).
[15] A. Grill and D. Itzhak, Thin Solid Films **101**, 219 (1983).
[16] L. Wang, X. Xu, Z. Yu, and Z. Hei, Surf. Coat. Technol. **124**, 93 (2000).
[17] M. P. Fewell, J. M. Priest, M. J. Baldwin, G. A. Collins, and K. T. Short, Surf. Coat. Technol. **131**, 284 (2000).
[18] S. Kumar, M. J. Baldwin, M. P. Fewell, S. C. Haydon, K. T. Short, G. A. Collins, and J. Tendys, Surf. Coat. Technol. **123**, 29 (2000).
[19] R. Günzel, M. Betzl, I. Alphonsa, B. Ganguly, P. I. John, and S. Mukherjee, Surf. Coat. Technol. **112**, 307 (1999).
[20] E. Menthe and K.-T. Rie, Surf. Coat. Technol. **116–119**, 199 (1999).
[21] M. Berg, C. V. Budtz-Jørgensen, H. Reitz, K. O. Schweitz, J. Chevallier, P. Kringhøj, and J. Bøttiger, Surf. Coat. Technol. **124**, 25 (2000).
[22] D. Hovorka, J. Vlček, R. Čerstvý, J. Musil, P. Bělský, and M. Růžička, J. Vac. Sci. Technol. A **18**, 2715 (2000).
[23] E. Camps, S. Muhl, S. Romero, and J. L. García, Surf. Coat. Technol. **106**, 121 (1998).
[24] N. Renevier, T. Czerwiec, P. Collignon, and H. Michel, Surf. Coat. Technol. **98**, 1400 (1998).
[25] M. Hudis, J. Appl. Phys. **44**, 1489 (1973).
[26] A. Ricard, J. Phys. D **30**, 2261 (1997).
[27] A. Szasz, D. J. Fabian, A. Hendry, and Z. Szaszne-Csih, J. Appl. Phys. **66**, 5598 (1989).
[28] J. M. Priest, M. J. Baldwin, and M. P. Fewell, Surf. Coat. Technol. **145**, 152 (2001).
[29] H. R. Kaufman, J. Vac. Sci. Technol. **15**, 272 (1978).
[30] P. W. Atkins, *Physical Chemistry*, 3rd ed. (Oxford University, England, 1986).
[31] P. Hammer, N. M. Victoria, and F. Alvarez, J. Vac. Sci. Technol. A **16**, 2941 (1998).
[32] Multi-Gauge Controller, Manual 6999-08-091, Revision U, December 1998. Varian Vacuum Tech., Lexinton, Mass.
[33] W. C. Oliver and G. M. Pharr, J. Mater. Res. **7**, 1564 (1992).
[34] W. Möller, S. Parascandola, O. Kruse, R. Günzel, and E. Richter, Surf. Coat. Technol. **116–119**, 1 (1999).
[35] R. Wei, Surf. Coat. Technol. **83**, 218 (1996).
[36] C. A. Figueroa, D. Wisnivesky, P. Hammer, R. G. Lacerda, R. Droppa, Jr., F. C. Marques, and F. Alvarez, Surf. Coat. Technol. **146–147**, 405 (2001).
[37] O. Öztürk and D. L. Williamson, J. Appl. Phys. **77**, 3839 (1995).
[38] S. Parascandola, O. Kruse, and W. Möller, Appl. Phys. Lett. **75**, 1851 (1999).
[39] S. Parascandola and W. Möller, Appl. Phys. Lett. **76**, 2194 (2000).
[40] P. Kizler, G. Frommeyer, and R. Rosenkranz, Z. Metallkd. **85**, 705 (1994).
[41] S. Sugiyama, H. Ohkubo, M. Takenaka, K. Ohsawa, M. I. Ansari, N. Tsukuda, and E. Kuramoto, J. Nucl. Mater. **283–287**, 863 (2000).
[42] B. Chapman, *Glow Discharge Processes* (Wiley-Interscience, New York, 1980).
[43] S. Parascandola, O. Kruse, E. Richter, and W. Möller, J. Vac. Sci. Technol. B **17**, 855 (1999).
[44] W. Möller, S. Parascandola, T. Telbizova, R. Günzel, and E. Richter, Surf. Coat. Technol. **136**, 73 (2001).
[45] X. Tian and P. K. Chu, J. Vac. Sci. Technol. A **19**, 1008 (2001).
[46] M. Johansson and L. G. Ekedahl, Appl. Surf. Sci. **180**, 27 (2001).
[47] F. Eisert, F. Gudmundson, and A. Rosen, Appl. Phys. B: Lasers Opt. **68**, 579 (1999).